

Structures and stabilities of doubly charged $(\text{MgO})_n\text{Mg}^{2+}$ ($n=1-29$) cluster ions

Andrés Aguado,^{a)} Francisco López-Gejo,^{b)} and José M. López

Departamento de Física Teórica, Facultad de Ciencias, Universidad de Valladolid, 47011, Valladolid, Spain

(Received 28 July 1998; accepted 8 December 1998)

Ab initio perturbed ion plus polarization calculations are reported for doubly charged nonstoichiometric $(\text{MgO})_n\text{Mg}^{2+}$ ($n=1-29$) cluster ions. We consider a large number of isomers with full relaxations of the geometries, and add the correlation correction to the Hartree–Fock energies for all cluster sizes. The polarization contribution is included at a semiempirical level also for all cluster sizes. Comparison is made with theoretical results for neutral $(\text{MgO})_n$ clusters and singly charged alkali–halide cluster ions. Our method is also compared to phenomenological pair potential models in order to assess their reliability for calculations on small ionic systems. The large coordination-dependent polarizabilities of oxide anions favor the formation of surface sites, and thus bulk-like structures begin to dominate only after $n=24$. The relative stabilities of the cluster ions against evaporation of an MgO molecule show variations that are in excellent agreement with the experimental abundance spectra. © 1999 American Institute of Physics. [S0021-9606(99)30610-3]

I. INTRODUCTION

Cluster science has become a field of intensive research both for experimentalists and theoreticians. Small aggregates have a fundamental interest because they provide a link between the molecular and the solid state physics; furthermore, they are important in new technological applications like nanoelectronics. Elucidating the structural and electronic properties of clusters remains a major challenge for present-day science, due to the significant deviations that clusters present in their physical and chemical properties when compared both to the molecule and the bulk. Another difficulty arises from the huge increase in the number of different isomers with cluster size. Many interesting cluster properties depend largely on the cluster structure, at least in the case of ionic and covalently bonded materials, so a complete description of the relevant isomer configurations for each cluster size is highly desirable.

In the last few years, considerable effort has been devoted to the understanding of metallic and semiconductor clusters. Meanwhile, studies on metal-oxide clusters have been comparatively scarce, despite of their fundamental role in important physical processes like heterogeneous catalysis. In this work, the interest is focused on magnesium oxide. Stoichiometric MgO clusters have been investigated both experimentally and theoretically. Saunders^{1,2} reported mass spectra and collision-induced-fragmentation data for sputtered $(\text{MgO})_n^+$ cluster ions, and Ziemann and Castleman^{3,4} performed experimental measurements by using laser-ionization time-of-flight mass spectrometry.^{5,6} Theoretical calculations have been performed at different levels of accu-

racy: simple ionic models based on phenomenological pair potentials⁷⁻⁹ were performed by Ziemann and Castleman⁴ to explain the global trends found in their experiments; Wilson¹⁰ has studied neutral $(\text{MgO})_n$ ($n \leq 30$) clusters by using a compressible-ion model¹¹ that includes coordination-dependent oxide polarizabilities;¹² semiempirical tight-binding calculations were reported by Moukouri and Noguera,^{13,14} and finally, *ab initio* calculations on stoichiometric MgO clusters were presented recently by Recio *et al.*,^{15,16} Malliavin and Coudray,¹⁷ and de la Puente *et al.*¹⁸ Nonstoichiometric $(\text{MgO})_n\text{Mg}^+$ and $(\text{MgO})_n\text{Mg}^{2+}$ cluster ions have been also detected and studied experimentally by Ziemann and Castleman.^{3,4,19} Specifically, they have obtained, by changing the flow rate of the carrier gas in a gas aggregation source, a mass spectrum comprised almost entirely of doubly charged $(\text{MgO})_n\text{Mg}^{2+}$ cluster ions.¹⁹ Enhanced stabilities in the small-size regime were found for $n=8, 11, 13, 16, 19, 22, 25$, and 27 , and were explained in terms of compact cubic clusters resembling pieces of the MgO crystal lattice. If we exclude the pair potential calculations performed by Ziemann and Castleman,^{4,19} there is no theoretical investigation of nonstoichiometric MgO cluster ions.

The “extra” cation present in nonstoichiometric cluster ions is expected to result in large structural distortions whenever a specially compact structure can not be constructed. That is not a problem in pair potential calculations, where the simplicity of the interactions allows for a complete geometrical relaxation of the different isomers at a very modest computational cost. Nevertheless, the need to use some selected set of empirical parameters for Mg^{q+} and O^{q-} ($q=1,2$) ions results in a serious questioning of the reliability of these simple ionic models. On the opposite side, traditional *ab initio* calculations based on the molecular orbital–linear combination of atomic orbitals approximation are very reli-

^{a)}Author to whom correspondence should be addressed. Electronic mail: aguado@jmlopez.fam.cie.uva.es

^{b)}Present address: Dept. of Physics and Astronomy, University College London, London WC1E 6BT, UK.

able but computationally expensive, the computer time requirements scaling with the fourth power of the number of atoms in the cluster. Thus, the calculations of Recio *et al.* on $(\text{MgO})_n$ and $(\text{MgO})_n^+$ clusters^{15,16} were performed under certain restrictions: (a) the geometries of most of the isomers were optimized with respect to a single parameter, namely the nearest-neighbor distance; (b) only two or three different isomers were considered for each cluster size; and (c) the correlation energy corrections (calculated at the MP2 level) were included only for $n \leq 6$. In the calculations of Malliavin and Coudray,¹⁷ the geometries were more carefully optimized but the results were limited to the size range $n = 1 - 6$.

In the present work, we report the results of an extensive and systematic study of $(\text{MgO})_n\text{Mg}^{2+}$ cluster ions with n up to 29. We have employed the *ab initio* perturbed ion (aiPI) model,²⁰ which is a Hartree–Fock model based on the theory of electronic separability^{21,22} and the *ab initio* model potential approach of Huzinaga *et al.*,²³ supplemented with some interaction energy terms to account for polarization contributions (see the next section). The model has been successfully employed by our group in several studies of alkali–halide clusters and cluster ions.^{24–28} It has been also used in a study of neutral stoichiometric $(\text{MgO})_n$ ($n = 1 - 13$) clusters.¹⁸ On one hand, our calculations represent a major advance with respect to pair potential methods, and on the other hand, they overcome most of the technical difficulties found in more sophisticated *ab initio* methods: (a) we have allowed for an appropriate geometrical relaxation of the isomers; (b) we have studied a large set of isomers for each cluster size (specifically, the total number of isomers studied is around 400); (c) correlation corrections, which have been proved to be essential for an accurate description of metal-oxide clusters,¹⁸ have been included for all cluster sizes; and (d) we have been able to study relatively large cluster sizes (up to $n = 29$), thus enlarging the usual size range covered by traditional *ab initio* methods.

The structural results presented in this work could also be useful in the interpretation of possible future experimental investigations on these clusters. By measuring the mobility of cluster ions through an inert buffer gas under the influence of a weak electric field, drift tube experimental studies provide valuable information about the cluster geometries.^{29–31}

The rest of the paper is organized as follows: in Sec. II we give a brief resume of the aiPI model as applied to clusters (full expositions of the method have been given elsewhere^{24,25}), a comparison with pair potential models which serves to assert the quality of the methodology, and the details of the computational procedure. The results are presented in Sec. III, and finally, Sec. IV summarizes the main conclusions extracted from this study.

II. THE aiPI MODEL: COMPARISON TO PAIR POTENTIAL MODELS

The *ab initio* perturbed-ion model²⁰ was originally designed for the description of ionic solids,³² and subsequently adapted to the study of clusters in our group.^{24–28} Its theoretical foundation lies in the theory of electronic separability,^{33,34} and its practical implementation in the

Hartree–Fock (HF) version of the theory of electronic separability.^{21,22} The HF equations of the cluster are solved stepwise, by breaking the cluster wave function into local group functions (ionic in nature, in our case). In each iteration, the total energy is minimized with respect to variations of the electron density localized in a given ion. The electron densities of the other ions are frozen. In the subsequent iterations, each frozen ion assumes the role of a nonfrozen ion. When the self-consistent process (see more details below) finishes, the outputs are the total cluster energy E_{clus} and a set of localized wave functions for each geometrically non-equivalent ion in the cluster. The cluster energy can be written as a sum of ionic additive energies^{24–26}

$$E_{\text{clus}} = \sum_{R=1}^N E_{\text{add}}^R, \quad (1)$$

where the sum runs over all ions in the cluster, and the contribution of each particular ion to the total cluster energy (E_{add}^R) can be expressed in turn as a sum of intraionic (net) and interionic contributions

$$E_{\text{add}}^R = E_{\text{net}}^R + \frac{1}{2} \sum_{S(\neq R)} E_{\text{int}}^{RS} = E_{\text{net}}^R + \frac{1}{2} E_{\text{int}}^R. \quad (2)$$

The localized nature of the aiPI procedure has some advantages over the usual molecular orbital models. As the correlation energy correction in weakly overlapping systems is almost intraionic in nature (being, therefore, a sum of contributions from each ion), the localized cluster-consistent ionic wave functions may be used to attain good estimations of this correction. In this paper, the correlation energy correction is obtained through Clementi's Coulomb–Hartree–Fock method.^{35,36} Besides, it also allows the development of computationally efficient codes³⁷ which make use of the large multizeta basis sets of Clementi and Roetti³⁸ for the description of the ions. In this respect, our optimizations have been performed using basis sets ($5s4p$) for Mg^{2+} and ($5s5p$) for O^{2-} , respectively. Inclusion of diffuse basis functions has been checked and shown to be unnecessary. Another advantage coming from the localized nature of the model is the linear scaling of the computational effort with the number of atoms in the cluster. This has allowed us to study clusters with as many as 59 atoms at a reasonable computational cost.

Self-consistency has been achieved in the following way: for a given distribution of the ions forming the cluster, we consider one of them as the active ion R (for instance, a particular oxygen anion), and solve the self-consistent-field equations for anion R in the field of the remaining ions, which are considered frozen at this stage. Next, we take another oxygen anion (anion S) as the active ion and repeat the same process. If the anion S is geometrically inequivalent to anion R , the energy eigenvalues and wave functions of electrons in anions S are different from those of anions R . We continue this process in the same way until all the anions have been exhausted. The same procedure is then followed for the magnesium cations. The process just described is a perturbed ion (PI) cycle. We iterate the PI cycles until convergence in the total energy of the cluster is achieved. Note

that the self-consistent process can be accelerated if equivalences between anions or cations are imposed by fixing the symmetry of an isomer. In order to allow for completely general distortions, we have not employed that simplification in the present study. Nevertheless, equivalences in some ionic wave functions have been observed at the end of the calculations for some highly symmetrical isomers.

It is very interesting to compare any quantum model designed for the study of ionic materials with the rigid ion and polarizable ion models.^{7–9} These pair potential models are very intuitive, and include in a phenomenological way all the relevant terms in the interatomic potential energy. The quality of an *ab initio* method developed for application on ionic materials can thus be assessed by specifying in which way it improves over a pair potential description. The binding energy in a pair potential model can be expressed as $E_{\text{bind}} = \frac{1}{2} \sum_{i \neq j} V_{ij} + \sum_i E_i^S$, where V_{ij} is the potential energy between ions i and j , and E_i^S is the self-energy of the ion i measured relative to the self-energy of the isolated atom. In the rigid ion model, we have⁹

$$V_{ij}^{\text{rigid}} = \frac{q_i q_j}{r_{ij}} + A_{ij} e^{-r_{ij}/\rho}, \quad E_i^{S,\text{rigid}} = 0. \quad (3)$$

The first term is the electrostatic Coulomb energy between two point ions with charges q_i and q_j , and the second term is the short-range repulsive Born–Mayer energy reflecting the mutual repulsion due to the overlap of the wave functions of the ions. In the polarizable ion model, a polarizability α_i is assigned to each ion so that the electron shells can be polarized by the electric field created by the other ions in the cluster. Now we have⁹

$$V_{ij}^{\text{pol}} = V_{ij}^{\text{rigid}} + V_{ij}^{MD} + V_{ij}^{DD}, \quad E_i^{S,\text{pol}} = \frac{\mu_i^2}{2\alpha}. \quad (4)$$

The self-energy is now different from zero, and the interaction energy contains two new terms: a monopole–dipole and a dipole–dipole interaction term. In the Born–Mayer repulsive potential, the distance r_{ij} is replaced by an effective value r_{ij}^{eff} to take into account the deformation of the electronic shells upon cluster formation. An intermediate pair potential model exists in which the repulsive radii of ions are allowed to deform isotropically under the effects of other ions in the system, but ionic polarizations arising from the positional displacements of each shell from its own core are not considered. This is the breathing shell model,³⁹ and constitutes an important improvement over the rigid ion model. Improvements over the basic polarizable-ion model have also been advanced by Madden and co-workers.⁴⁰ In the aiPI model, the binding energy can be written as a sum of ionic contributions, which are in turn expressed as a sum of deformation and interaction terms^{24–26}

$$E_{\text{bind}} = \sum_R E_{\text{bind}}^R = \sum_R (E_{\text{def}}^R + \frac{1}{2} E_{\text{int}}^R). \quad (5)$$

The interaction energy term is of the form

$$E_{\text{int}}^R = \sum_{S \neq R} E_{\text{int}}^{RS} = \sum_{S \neq R} (E_{\text{class}}^{RS} + E_{\text{nc}}^{RS} + E_X^{RS} + E_{\text{overlap}}^{RS}), \quad (6)$$

where the different energy contributions are: the classical electrostatic interaction energy between point-like ions; the correction to this energy due to the finite extension of the ionic wave functions; the exchange interaction energy between the electrons of ion R and those of the other ions in the cluster; and the overlap repulsive energy contribution.³⁴ The deformation energy term E_{def}^R is the self-energy of the ion R measured relative to the self-energy of the isolated ion. It is an intrinsically quantum-mechanical many-body term that accounts for the energy change associated with the compression of the ionic wave functions upon cluster formation, and incorporates the correlation contribution to the binding energy. All those terms are calculated in an *ab initio* self-consistent way. Thus, the improvement over the classical rigid-ion description is clear. Improvement over a polarizable-ion description can be questionable in principle due to one basic assumption used in the actual code, namely spherically symmetric electron densities, centered on the nuclei. The electron density clouds of the ions are thus allowed to distort just isotropically under the effect of the other ions in the cluster, and indeed the aiPI model could be considered as an *ab initio* breathing shell model. In summary, although the aiPI method treats quantum-mechanically all the terms present in a breathing shell model, plus other many-body terms absent from any classical model, it does not describe the dipolar terms present in a polarizable-ion model because there are no induced dipoles. In our previous works on alkali–halide clusters,^{24–28} inclusion of polarization was not considered essential. However, the O^{2-} anion has a very deformable density cloud (that is, a large coordination-dependent polarizability), and dipolar contributions are expected to be more important than for halide anions. Relaxing the spherical symmetry assumption would allow in principle for a proper description of those terms, but many of the computational advantages of the aiPI model (which have allowed us to perform such a detailed study) would be lost. The solution we have chosen is to include the polarization terms in the self-consistent process with an extended polarizable point-ion description.¹⁰ In such a way, the “enlarged” model obtained improves clearly over all classical descriptions, and can be considered a benchmark for the pair potential calculations. The price to be paid is the inclusion of parametrized coordination-dependent polarizabilities for the ions. However, the polarizabilities that are introduced as parameters in the calculations have been obtained from accurate *ab initio* calculations,¹² and thus the reliability of the model is reduced just a little compared to the most sophisticated *ab initio* methods, whereas complete geometrical distortions can be considered and a large number of isomers studied at less cost. Furthermore, the only cases in which doubts related to the energetical ordering of the isomers arise are those showing near-degenerate isomers, and we will show that those situations are not frequent.

Now, we explain the calculational method used in our study of $(\text{MgO})_n \text{Mg}^{2+}$ cluster ions. We had no knowledge *a priori* as to what shapes these clusters can adopt. So, we performed an extensive sampling of the potential energy surface by generating a large set of random cluster configurations for each cluster size n with $n = 1–13$. Except for the

smallest sizes ($n=1,2$), typically 100 000 configurations were generated for each n . All those random configurations were fully optimized by using a rigid-ion model. The parameters in Eq. (3) were those used by Ziemann and Castleman,^{4,19} although some tests were also performed with the set of parameters of Bush *et al.*⁴¹ Both sets of parameters led to essentially identical structures, differing just in minor details. These pair potential calculations could be performed at a low computational cost, and therefore were very useful in locating reasonable initial guesses for the different minima on the potential energy surface. Then, we typically took the 15–20 lowest-energy isomers obtained in the pair potential calculations for each cluster size as input geometries for the aiPI calculations. We also studied structures obtained by adding or removing in different ways a molecule from those pair-potential structures, of course whenever such a structure was not already present in the pair-potential results. Most of the structures obtained in the range $n=1-13$ could be classified as $a \times b \times c$, where a , b , and c indicate the number of atoms along three perpendicular edges, so for $n > 13$ we directly studied geometries with that formula. We have also considered stackings of the different planar structures found for $n \leq 13$. While we can not rule out completely the possibility of having overlooked some important isomer, we believe that we have reduced it considerably. We have performed aiPI+polarization calculations on all those isomers, without considering any equivalence between the ions. The optimizations of the geometries have been performed by using a downhill simplex algorithm.^{42,43} For the oxide polarizabilities we have used the values given by Wilson.¹⁰ The magnesium polarizability is taken equal to the bulk value.⁴⁴

We finish this section with a comment about the ionic character of our model. Although the aiPI model describes the MgO cluster ions in terms of Mg^{2+} and O^{2-} units, we would like to stress that it does not enter in conflict with any possible assignment of fractional charges to each ion in *classical* models. In fact, the charges used by Ziemann and Castleman^{4,19} were ± 1 , the charges in the potential of Bush *et al.*⁴¹ are ± 2 , and both potentials give very similar results. The difference in the Coulomb part is compensated by a difference in the repulsive part. In other words, those charges are just parameters. On the other hand, ionic charges can be derived from quantum-mechanical calculations following the ideas of Bader.⁴⁵ That has been done recently in aiPI calculations on ionic solids from which fractional ionic charges have been derived.⁴⁶ Moreover, Wilson¹⁰ and Madden and co-workers⁴⁰ have shown that an extended ionic model including accurate polarization terms can account for several effects traditionally attributed to “covalency.” Bulk MgO is excellently described by the aiPI model,⁴⁷ and our aiPI plus polarization results for the MgO molecule bond length and vibrational frequency are $d=1.77 \text{ \AA}$ and $\omega=737 \text{ cm}^{-1}$, in good agreement with experiment⁴⁸ and *ab initio* methods.^{15,17} The appropriateness of the method for the study of metal oxide clusters is thus assessed.

III. RESULTS

A. Ground state structures and low-lying isomers

In the following, we restrict our discussion to the structural properties of the lowest-lying isomers. The $(\text{MgO})_n \text{Mg}^{2+}$ aiPI+polarization structures are shown in Fig. 1. The ground state (GS) and one or two low-lying isomers are given for each n , except for $n \geq 24$, where only one isomer is shown. A cutoff of 2.54 \AA , that exceeds by $\approx 20\%$ the Mg–O distance in the bulk, was arbitrarily chosen in order to decide whether an O atom is bonded to an Mg neighbor or not. The energy difference with respect to the most stable isomer is given (in eV) below each isomer. For cluster sizes $n=1$ and $n=2$ (not shown in the figure), a chain is obtained as the most stable isomer. The emergence of the bulk crystalline structure can be appreciated from Fig. 1: one-dimensional chains are observed for the smallest cluster sizes ($n=1-2$); a planar two-dimensional structure is the GS for $n=3$; next, there is a size region ($n=4-17$) in which three-dimensional (3D) structures are already predominant, but without an establishment of the bulk symmetry. Specifically, all the ions in those structures are in surface-like sites. The establishment of face-centered cubic structures starts at $n=18$, but is not complete until $n=24$. From that value on, all the ground state isomers are fragments of a rocksalt lattice.

Let us describe now in more detail the structures obtained as a function of n , first for the small cluster sizes ($n < 17$). Linear chains are the most stable isomers for $n=1$ and $n=2$. The $n=3$ GS is a planar rectangular structure with a cation attached to a corner. A structure obtained by removing an anion from a perfect cube appears 5.12 eV above, and a chain is observed as well as a noncompetitive isomer. The first three-dimensional ground state isomer occurs for $n=4$. It is obtained by adding a cation to an $(\text{MgO})_4$ cubic cluster. A quasiplanar 3×3 sheet and the chain are not competitive anymore. For $n=5$, a $2 \times 2 \times 3$ piece with an anion removed from a corner is obtained as the ground state isomer. From $n=5$ to $n=17$, all the ground state isomers are obtained by adding an MgO molecule either to the GS or to a low-lying isomer of the $(\text{MgO})_{n-1} \text{Mg}^{2+}$ cluster, in such a way that no bulk ions (ions with coordination of 6) are present. The formation of surface sites (with coordination equal to 3, 4, or 5) is favored instead. This is a direct consequence of the larger polarizabilities of oxide anions with lower coordinations. The minimization of just the electrostatic Coulomb energy between point ions would lead to the formation of more compact bulk-like structures, for which the ions would tend to attain its full first-coordination sphere. But when polarization effects are included, the dipole stabilization energy has to be minimized also, favoring a reduction of the coordination number and the formation of surface sites, the same conclusion achieved by Wilson¹⁰ in his study of neutral $(\text{MgO})_n$ clusters. As a result that is really worth mentioning, the GS structure for $n=13$ is not a $3 \times 3 \times 3$ perfect cube; that is what one would have “expected” by comparing with the situation encountered for alkali–halide cluster ions.^{27,28,31} This essentially different structural behavior has its roots in the increased polarizability of the oxide compared to halide

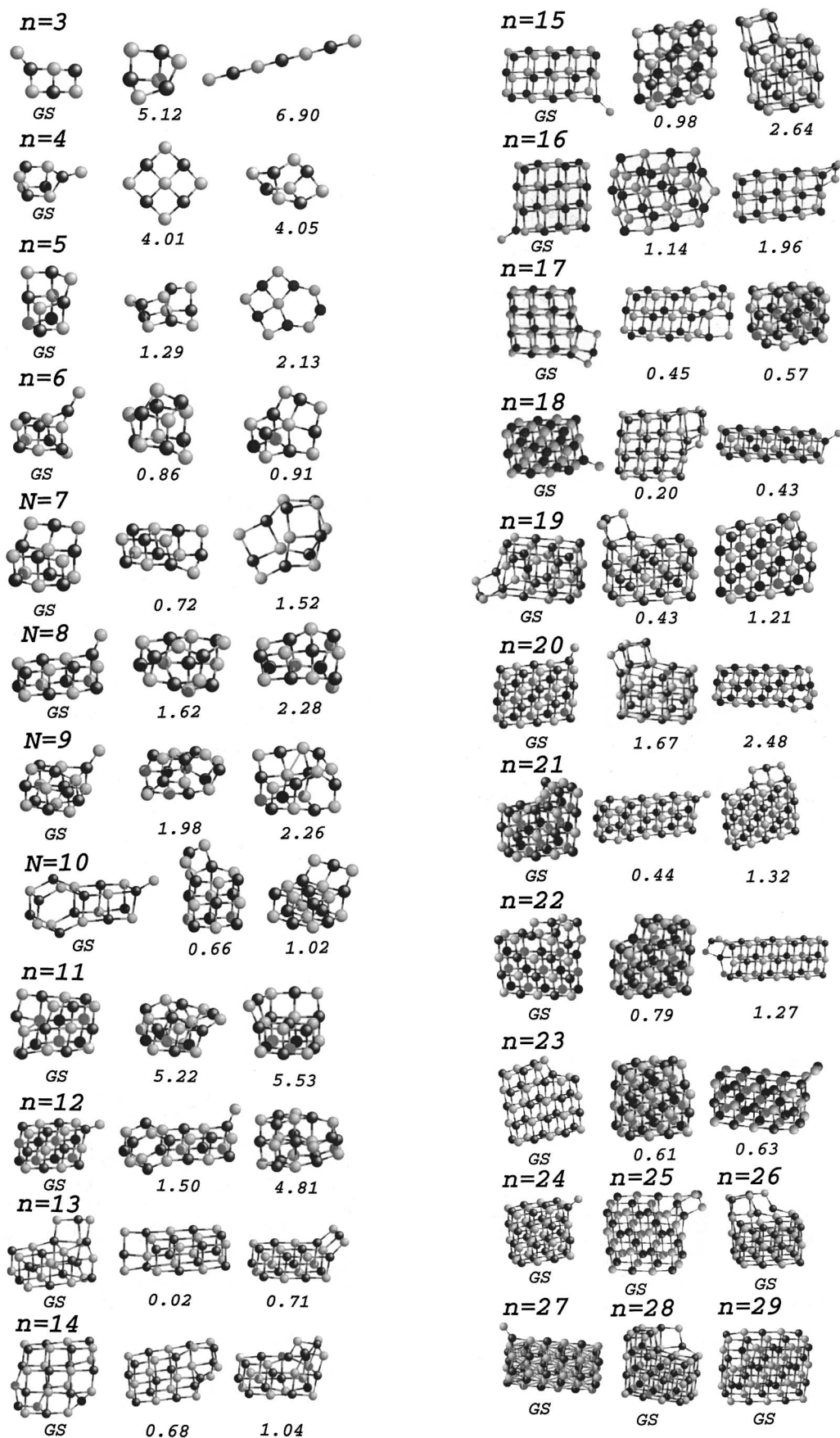


FIG. 1. Lowest-energy structure and low-lying isomers of $(\text{MgO})_n\text{Mg}^{2+}$ cluster ions. Light circles are Mg^{2+} cations and dark circles are O^{2-} anions. The energy difference (in eV) with respect to the most stable structure is given below the corresponding isomers. For $n \geq 24$, only the ground state isomer is shown.

anions, and can be accounted for by an enlarged ionic model like the one used here, without resorting to the inclusion of covalent effects.^{10,40} The $3 \times 3 \times 3$ $(\text{MgO})_{13}\text{Mg}^{2+}$ isomer has an oxide anion with coordination of 6, so with a small polarizability. Moreover, the corner sites of that isomer are occupied by cations, so there is no oxide anion with coordination of 3. All this results in a small polarization contribution to the energy that is not compensated by the increased Madelung energy.

Eventually, there has to be a cluster size where bulk-like fragments begin to dominate. The situation changes a little at $n=18$, where a ground state isomer with bulk-like ions appears for the first time, specifically a $3 \times 3 \times 4$ cubic structure with a cation attached to a corner. Let us note that a major difference between this structure and the $3 \times 3 \times 3$ $(\text{MgO})_{13}\text{Mg}^{2+}$ isomer is that now there are oxide anions in corner positions which enhance the polarization contribution. This enhancement, together with the increased Madelung term associated with a bulk-like fragment, make that isomer more stable than the one obtained by adding an MgO molecule to the $(\text{MgO})_{17}\text{Mg}^{2+}$ ground state. The establishment of bulk-like symmetry is not complete yet, however. For $n=19$, a $3 \times 3 \times 4$ structure with three ions attached is still favored, even more than for $n=18$, because now none of the four oxide anions with coordination of 3 is capped by a magnesium. By adding five ions to such a cubic structure, however, at least two oxide anions in corner sites are capped, and so the GS structure of $(\text{MgO})_{20}\text{Mg}^{2+}$ is again an isomer with only surface sites. For $n=22$, a $3 \times 3 \times 5$ perfect structure can be formed, in analogy with the case of $n=13$. Such a structure would have no oxide anions in corner positions and two oxides with coordination of 6, however, and it is still not energetically favored. From $n=24$ on, all the structures obtained are fragments of a bulk-like crystalline lattice. Although it is possible that for some larger cluster size the ground state structure will not yet be the most compact face-centered cubic fragment, we think we can accept with relative safety $n=24$ as the critical size where bulk-like symmetry emerges. This is consistent with the critical size ($n=30$) estimated by Wilson¹⁰ for neutral $(\text{MgO})_n$ clusters.

Our conclusions suggest substantial structural differences between $(\text{MgO})_n\text{Mg}^{2+}$ cations and $(\text{MgO})_n\text{O}^{2-}$ anions. For example, the perfect $3 \times 3 \times 3$ cube isomer of $(\text{MgO})_{13}\text{O}^{2-}$ would not have any oxide anion with coordination of 6, and all eight corner sites would be occupied by oxides. The case of $3 \times 3 \times 5$ $(\text{MgO})_{22}\text{O}^{2-}$ isomer would be similar. We have performed additional calculations for those two cluster sizes, and have obtained the $3 \times 3 \times 3$ and $3 \times 3 \times 5$ fragments as ground state isomers of $(\text{MgO})_{13}\text{O}^{2-}$ and $(\text{MgO})_{22}\text{O}^{2-}$, respectively.

A comparison with the results obtained for alkali-halide cluster ions^{27,28} and neutral $(\text{MgO})_n$ clusters^{10,18} is illustrative. Hexagonal prismatic structures are very common for $(\text{MgO})_n$ clusters,^{10,18} as well as for some neutral alkali-halide $(\text{AX})_n$ clusters.²⁴⁻²⁶ However, cubic structures are clearly predominant for $(\text{MgO})_n\text{Mg}^{2+}$ cluster ions, this being the main effect of nonstoichiometry and net charge: (a) perfect cubic structures can be built up with an odd number of ions, but an even number of ions is needed to construct a

perfect hexagonal prism; and (b) for “defectlike” structures, the extra charge is screened more effectively in the cuboid-like isomers. Examples can be found at $n=3$, where the hexagonal $(\text{MgO})_3$ isomer¹⁸ converts into a rectangular structure upon adding Mg^{2+} to lower the repulsion between cations, and at $n=10$, where adding a triatomic Mg-O-Mg to the hexagonal prism of the neutral $(\text{MgO})_9$ (Ref. 18) results in an isomer less stable than that obtained by adding Mg-O-Mg to a rocksalt piece (second isomer in Fig. 1). Let us now compare with the results obtained for alkali-halide cluster ions.^{27,28} The main difference comes from the polarization contribution. As stated above, this is less important in alkali-halide materials, for which the establishment of bulk-like symmetry is already complete at $n=13$. There is just another minor difference: centered structures, containing an inner alkali cation with high coordination, were found frequently for $(\text{NaI})_n\text{Na}^+$ and $(\text{CsI})_n\text{Cs}^+$, but such isomers are not observed for $(\text{MgO})_n\text{Mg}^{2+}$. Evidently, the repulsion between oxide anions is larger than the repulsion between halide anions, and allocating six O^{2-} anions around an Mg^{2+} cation is energetically less favorable.

We finish this section with a discussion of the validity of pair potential models and the effects of the polarization correction on cluster structure. Comparison of our pair potential calculations with the aiPI results leads us to the following two important points: (a) pair potential models fail to reproduce quantitatively the expansion of the interionic distances with cluster size; and (b) the energetical ordering of the different isomers for a given cluster size is not reliable. On the positive side, the shape of the isomers is usually quite well reproduced, and the main structural correction obtained with an aiPI calculation is a global scaling of all the interionic distances. This last observation supports the use of pair potentials to locate good initial configurations for ionic clusters, from which *ab initio* calculations can be started. The effects of the polarization correction are sizable for $n < 17$. The correct determination of the ground states would not be achieved with a model that did not include polarization corrections, as surface sites would not be specially favored. Moreover, for the smallest cluster sizes ($n < 8$), the dimensionality of the isomers is not reproduced either. Specifically, linear chains are the GS isomers for $n=1-3$, and planar structures are the most stable isomers for $n=4-7$ in aiPI calculations without polarization. Thus, inclusion of polarization speeds up the emergence of 3D structures. The imprecisions associated with the lack of polarization corrections turn smaller as the cluster size increases and bulk-like fragments begin to dominate.

B. Relative stabilities: Comparison to experimental results

In order to study the relative stabilities of $(\text{MgO})_n\text{Mg}^{2+}$ cluster ions, we calculate the evaporation threshold energy^{9,28} required to remove an MgO molecule from the ground state isomer. For a cluster $(\text{MgO})_n\text{Mg}^{2+}$, this is done as follows: we consider the optimized GS structure and identify the MgO molecule that contributes the least to the cluster binding energy. Then we remove that molecule and relax the resulting $(\text{MgO})_{n-1}\text{Mg}^{2+}$ fragment to the nearest local mini-

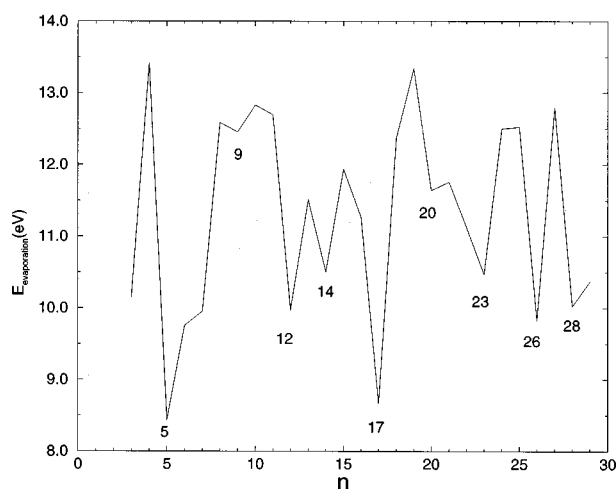


FIG. 2. Evaporation threshold energies required to remove a neutral MgO molecule from $(\text{MgO})_n\text{Mg}^{2+}$ cluster ions as a function of n . The local minima in the evaporation energy curve are shown explicitly.

num. The total energy required to evaporate a molecule is then the difference between the energy of the parent cluster and the energies of the two fragments, one of which is the MgO molecule

$$E_{\text{evaporation}}(n) = E_{\text{cluster}}[(\text{MgO})_{n-1}\text{Mg}^{2+}] + E(\text{MgO}) - E_{\text{cluster}}[(\text{MgO})_n\text{Mg}^{2+}]. \quad (7)$$

This process can be termed locally adiabatic because both fragments are allowed to relax to the local minimum energy configuration after the evaporation. For some cluster sizes, the fragment of size $(n-1)$ left when an MgO molecule is removed from $(\text{MgO})_n\text{Mg}^{2+}$ does not lie on the catchment basin of the $(\text{MgO})_{n-1}\text{Mg}^{2+}$ GS isomer, so that the evaporation threshold energies are larger than the energy differences between adjacent ground states minus $E(\text{MgO})$ in those cases. The evaporation energies are plotted as a function of n in Fig. 2. In the experiments performed by Ziemann and Castleman,¹⁹ the abundances in the mass spectra reflect the relative stabilities of $(\text{MgO})_n\text{Mg}^{2+}$ cluster ions against evaporation of an MgO molecule. Starting from the largest cluster size studied, we can appreciate minima in Fig. 2 for $n=28, 26, 23, 20, 17, 14, 12, 9,$ and 5 . Thus, evaporation of an MgO molecule from those clusters is easy relative to evaporation from clusters of other sizes. Moreover, the curve shows abrupt increases precisely at those cluster sizes, so that evaporation of an MgO molecule from the clusters of size $(n-1)$ is significantly more expensive than evaporation from cluster ions of size n . All of this results in an enrichment of $(\text{MgO})_n\text{Mg}^{2+}$ clusters with $n=4, 8, 11, 13, 16, 19, 22, 25,$ and 27 , a result which is in complete agreement with the experiment.¹⁹ Nevertheless, there is not a total correspondence between the experimental magic numbers and maxima in the evaporation energy curve. The experimental enhanced abundances result from a balance between two main processes: (a) evaporation from clusters with size $(n+1)$ results in an enrichment of the $(\text{MgO})_n\text{Mg}^{2+}$ clusters; and (b) evaporation from clusters with size n has the opposite effect.

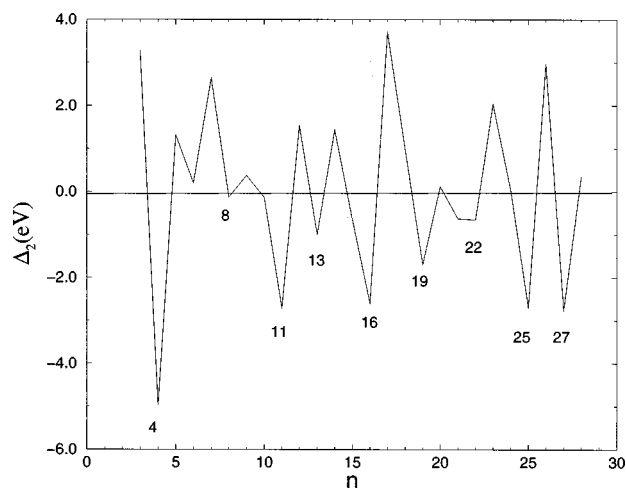


FIG. 3. Second derivative $\Delta_2(n)$ for $(\text{MgO})_n\text{Mg}^{2+}$ cluster ions as a function of the cluster size. Minima identify those cluster sizes with an enhanced relative stability.

A quantity that measures the stability of an $(\text{MgO})_n\text{Mg}^{2+}$ cluster ion relative both to $(\text{MgO})_{n+1}\text{Mg}^{2+}$ and $(\text{MgO})_{n-1}\text{Mg}^{2+}$ cluster ions is thus

$$\Delta_2(n) = E_{\text{evaporation}}(n+1) - E_{\text{evaporation}}(n), \quad (8)$$

where both terms in the difference are calculated using Eq. (7) as explained above. This quantity is plotted as a function of n in Fig. 3. Minima are apparent at $n=4, 8, 11, 13, 16, 19, 22, 25,$ and 27 . Thus, the experimental results concerning enhanced relative stabilities are properly reproduced by our calculations.

Opposite to the case of alkali-halide clusters²⁶ and cluster ions,²⁸ the magic numbers observed for $(\text{MgO})_n\text{Mg}^{2+}$ cannot be clearly explained in terms of a compactness argument. Instead, all the magic numbers observed verify the following: when removing the least bound MgO molecule from $(\text{MgO})_n\text{Mg}^{2+}$ (where n is a magic number), the resulting $(\text{MgO})_{n-1}\text{Mg}^{2+}$ is never in the catchment area of the ground state isomer, and thus the evaporation energy is large. Let us note that in some cases ($n=13, 19, 25$) this is not a direct consequence of the shape of the ground state isomers involved, but of the asymmetry between the different facets of those isomers, which make it energetically more favorable to allocate three ‘‘extra’’ ions on a different facet than one extra ion. Moreover, the magic numbers ($n=4, 11, 13, 16, 22, 25, 27$) verify a second property: when removing the least bound MgO molecule from $(\text{MgO})_{n+1}\text{Mg}^{2+}$ (where n is again a magic number), the resulting $(\text{MgO})_n\text{Mg}^{2+}$ structure is either the ground state structure or a low-lying isomer, and thus the evaporation energy shows a local minimum for those cluster sizes. Although there is a striking periodicity of 3 in the magic numbers observed between $n=13$ and $n=27$, our results indicate that there is not any special structural motif behind that periodicity.

IV. SUMMARY

The *ab initio* perturbed-ion model, supplemented with a semiempirical treatment of dipolar terms, has been employed

in order to study the structural and energetic properties of $(\text{MgO})_n\text{Mg}^{2+}$ ($n=1-29$) cluster ions. We have used a rigid ion model to generate a large set of initial configurations for each cluster size. Next, those structures have been optimized without considering any equivalence between different ions, thus allowing for an appropriate geometrical relaxation. Correlation corrections, which turned out to be essential for a proper description of $(\text{MgO})_n$ clusters,¹⁸ have been added to the Hartree-Fock energies for all cluster sizes. Inclusion of parametrized coordination-dependent polarizabilities reduces just a little the reliability of the model compared to full *ab initio* methods, because those polarizabilities have been extracted themselves from accurate *ab initio* calculations, and allows us to perform such a systematic study with appropriate geometrical relaxations at a significantly reduced computational cost. The structural trends of $(\text{MgO})_n\text{Mg}^{2+}$ cluster ions have been described. The emergence of the bulk crystalline symmetry proceeds in different stages, from one-dimensional configurations for $n=1-2$ to a planar structure for $n=3$, and then to three-dimensional structures with a clear predominance of cubic structures with surface sites for $n=4-17$. The critical size at which bulk-like rocksalt fragments dominate the spectrum is $n=24$. For $(\text{MgO})_{13}\text{Mg}^{2+}$ and $(\text{MgO})_{22}\text{Mg}^{2+}$, the “expected” $3\times 3\times 3$ and $3\times 3\times 5$ rocksalt isomers are neither the ground states nor low-lying isomers. This, at first sight surprising, result has been rationalized in terms of the importance of the polarization contribution, and the preference of oxide anions for surface-like (especially corner) sites. A comparison with the structures obtained for neutral $(\text{MgO})_n$ clusters^{10,18} shows that the preference for cuboid-like structures is a direct consequence of nonstoichiometry and net charge. Comparison with the structures obtained for alkali-halide cluster ions²⁸ reveals substantial differences that can be explained in terms of the larger polarizabilities of oxide anions compared to halide anions, and to a lesser extent in terms of the larger repulsion between oxide anions compared to the repulsion between halide anions. The main effects of the polarization correction are to speed up the emergence of 3D structures, to lower the average coordination, and to favor the formation of surface sites. Once bulklike structures are well established, polarization plays a less important role.

The relative stabilities of $(\text{MgO})_n\text{Mg}^{2+}$ cluster ions have been studied by calculating the energy required to evaporate an MgO molecule from the GS structures and the first differences between those evaporation energies, that reflect the stability of a cluster of size n relative to the stabilities of the neighbor clusters of sizes $(n+1)$ and $(n-1)$. Both sets of calculations predict the clusters with $n=4, 8, 11, 13, 16, 19, 22, 25,$ and 27 to be especially stable, a result that is in complete agreement with the experimental enhanced abundances reported by Ziemann and Castleman.¹⁹ The interpretation of the enhanced stabilities in terms of highly compact fragments of a face-centered cubic crystalline lattice is not appropriate for such small clusters. Those enhanced stabilities have been explained in terms of an analysis of the evaporation process, which involves the explicit consideration of isomer structures different from the ground states.

Finally, a comparison has been made with the results

obtained by using a phenomenological pair potential model. This comparison has shown that, while pair potential calculations are quite helpful when obtaining initial guesses for the isomer geometries, the distances and the energetical ordering of the isomers obtained with them are generally not reliable.

ACKNOWLEDGMENTS

The authors gratefully acknowledge Professor J. D. Gale for providing us with a copy of Ref 42 and Professor A. W. Castleman, Jr. for discussing with us the experimental results in Ref. 19. Work supported by DGES (PB95-0720-C02-01) and Junta de Castilla y León (VA63/96). A. Aguado is supported by a predoctoral fellowship from Junta de Castilla y León.

- ¹W. A. Saunders, Phys. Rev. B **37**, 6583 (1988).
- ²W. A. Saunders, Z. Phys. D **12**, 601 (1989).
- ³P. J. Ziemann and A. W. Castleman, Jr., Z. Phys. D **20**, 97 (1991).
- ⁴P. J. Ziemann and A. W. Castleman, Jr., J. Chem. Phys. **94**, 718 (1991).
- ⁵C. W. S. Conover, Y. A. Yang, and L. A. Bloomfield, Phys. Rev. B **38**, 3517 (1988).
- ⁶Y. T. Twu, C. W. S. Conover, Y. A. Yang, and L. Bloomfield, Phys. Rev. B **42**, 5306 (1990).
- ⁷T. P. Martin, Phys. Rep. **95**, 168 (1983).
- ⁸J. Diefenbach and T. P. Martin, Surf. Sci. **156**, 234 (1984).
- ⁹N. G. Phillips, C. W. S. Conover, and L. A. Bloomfield, J. Chem. Phys. **94**, 4980 (1991).
- ¹⁰M. Wilson, J. Phys. Chem. B **101**, 4917 (1997).
- ¹¹M. Wilson, P. A. Madden, N. C. Pyper, and J. H. Harding, J. Chem. Phys. **104**, 8068 (1996).
- ¹²P. W. Fowler and P. Tole, Surf. Sci. **197**, 457 (1988); P. Jemmer, P. W. Fowler, M. Wilson, and P. A. Madden, J. Phys. Chem. A **102**, 8377 (1998), and references therein.
- ¹³S. Moukouri and C. Noguera, Z. Phys. D **24**, 71 (1992).
- ¹⁴S. Moukouri and C. Noguera, Z. Phys. D **27**, 79 (1993).
- ¹⁵J. M. Recio and R. Pandey, Phys. Rev. A **47**, 2075 (1993).
- ¹⁶J. M. Recio, R. Pandey, A. Ayuela, and A. B. Kunz, J. Chem. Phys. **98**, 4783 (1993).
- ¹⁷M. J. Malliavin and C. Coudray, J. Chem. Phys. **106**, 2323 (1997).
- ¹⁸E. de la Puente, A. Aguado, A. Ayuela, and J. M. López, Phys. Rev. B **56**, 7607 (1997).
- ¹⁹P. J. Ziemann and A. W. Castleman, Jr., Phys. Rev. B **44**, 6488 (1991).
- ²⁰V. Luña and L. Pueyo, Phys. Rev. B **41**, 3800 (1990).
- ²¹S. Huzinaga and A. A. Cantu, J. Chem. Phys. **55**, 5543 (1971).
- ²²S. Huzinaga, D. McWilliams, and A. A. Cantu, Adv. Quantum Chem. **7**, 183 (1973).
- ²³S. Huzinaga, L. Seijo, Z. Barandiarán, and M. Klobukowski, J. Chem. Phys. **86**, 2132 (1987).
- ²⁴A. Ayuela, J. M. López, J. A. Alonso, and V. Luña, Z. Phys. D **26**, S213 (1993); An. Fis. **90**, 190 (1994); Physica B & C **212**, 329 (1996).
- ²⁵A. Aguado, A. Ayuela, J. M. López, and J. A. Alonso, J. Phys. Chem. B **101**, 5944 (1997).
- ²⁶A. Aguado, A. Ayuela, J. M. López, and J. A. Alonso, Phys. Rev. B **56**, 15353 (1997).
- ²⁷A. Ayuela, J. M. López, J. A. Alonso, and V. Luña, Can. J. Phys. **76**, 311 (1998).
- ²⁸A. Aguado, A. Ayuela, J. M. López, and J. A. Alonso, Phys. Rev. B **58**, 9972 (1998).
- ²⁹G. von Helden, M. T. Hsu, P. R. Kemper, and M. T. Bowers, J. Chem. Phys. **95**, 3835 (1991).
- ³⁰M. F. Jarrold, J. Phys. Chem. **99**, 11 (1995).
- ³¹M. Maier-Borst, P. Löffler, J. Petry, and D. Kreisle, Z. Phys. D **40**, 476 (1997).
- ³²V. Luña, M. Flórez, E. Francisco, A. Martín Pendás, J. M. Recio, M. Bermejo, and L. Pueyo, in *Cluster Models for Surface and Bulk Phenomena*, edited by G. Pacchioni, P. S. Bagus, and F. Parmigiani (Plenum, New York, 1992), p. 605.

- ³³R. McWeeny, *Methods of Molecular Quantum Mechanics* (Academic, London, 1994).
- ³⁴E. Francisco, A. Martín Pendás, and W. H. Adams, *J. Chem. Phys.* **97**, 6504 (1992).
- ³⁵E. Clementi, *IBM J. Res. Dev.* **9**, 2 (1965).
- ³⁶S. J. Chakravorty and E. Clementi, *Phys. Rev. A* **39**, 2290 (1989).
- ³⁷V. Luaña, A. Martín Pendás, J. M. Recio, and E. Francisco, *Comput. Phys. Commun.* **77**, 107 (1993).
- ³⁸E. Clementi and C. Roetti, *At. Data Nucl. Data Tables* **14**, 177 (1974).
- ³⁹M. Matsui, *J. Chem. Phys.* **108**, 3304 (1998).
- ⁴⁰P. A. Madden and M. Wilson, *Chem. Soc. Rev.* **25**, 399 (1996); A. J. Rowley, P. Jemmer, M. Wilson, and P. A. Madden, *J. Chem. Phys.* **108**, 10209 (1998).
- ⁴¹T. S. Bush, J. D. Gale, C. R. A. Catlow, and P. D. Battle, *J. Mater. Chem.* **4**, 831 (1994).
- ⁴²J. A. Nelder and R. Mead, *Comput. J. (UK)* **7**, 308 (1965).
- ⁴³W. H. Press and S. A. Teukolsky, *Comput. Phys.* **5**, 426 (1991).
- ⁴⁴P. W. Fowler and N. C. Pyper, *Proc. R. Soc. London, Ser. A* **398**, 377 (1985).
- ⁴⁵R. F. W. Bader, *Atoms in Molecules* (Oxford University Press, Oxford, 1990).
- ⁴⁶A. Martín Pendás, A. Costales, and V. Luaña, *Phys. Rev. B* **55**, 4275 (1997); V. Luaña, A. Costales, and A. Martín Pendás, *ibid.* **55**, 4285 (1997); A. Martín Pendás, A. Costales, and V. Luaña, *J. Phys. Chem. B* **102**, 6937 (1998).
- ⁴⁷V. Luaña, J. M. Recio, and L. Pueyo, *Phys. Rev. B* **42**, 1791 (1990).
- ⁴⁸K. P. Huber and G. Herzberg, *Molecular Spectra and Molecular Structure IV. Constants of Diatomic Molecules* (Van Nostrand Reinhold, Princeton, NJ, 1979).